Scientia Horticulturae 276 (2021) 109763

Contents lists available at ScienceDirect

Scientia Horticulturae

journal homepage: www.elsevier.com/locate/scihorti

Leaf physiological impedance and elasticity modulus in *Orychophragmus violaceus* seedlings subjected to repeated osmotic stress

Deke Xing [a,c], Lu Chen [a], Yanyou Wu [b,*], Janusz J. Zwiazek [c]

[a] Key Laboratory of Modern Agricultural Equipment and Technology, Ministry of Education, Institute of Agricultural Engineering, Jiangsu University, 212013, Zhenjiang, PR China

[b] Research Center for Environmental Bio-Science and Technology, State Key Laboratory of Environmental Geochemistry, Institute of Geochemistry, Chinese Academy of Sciences, 550081, Guiyang, PR China

[c] Department of Renewable Resources, University of Alberta, Edmonton, AB, T6G 2E3, Canada

ARTICLE INFO

Keywords:
Carbonic anhydrase
Cell stiffness
Leaf water dissipation rate
Photosynthesis
Re-watering water-use efficiency

ABSTRACT

Leaf water status is always influenced by plant growth and environment and dynamically changes over time. Rapid measurement of leaf physical characteristics helps to timely determine the plant water needs, in order to prevent inhibition of photosynthesis in plants and improve irrigation water-use efficiency (WUE) under water deficit conditions. The present study determined leaf electrophysiological and mechanical properties, water content (LWC), water potential (Ψ_L), carbonic anhydrase (CA) activity, net photosynthesis, and re-watering WUE (WUE_R) in relation to osmotic stress and following drought hardening in *Orychophragmus violaceus* seedlings. The study established a coupling model between gripping force and physiological impedance according to the Nernst equation, and the leaf water dissipation rate (LWDR) was defined and determined. Changes of cell stiffness and LWDR altered the intracellular water status, which affected the photosynthetic capacity and WUE_R. Photosynthesis was inhibited by the 40 g L^{-1} PEG (polyethylene glycol) treatment due to the reduction of intracellular water, and leaf cells were severely damaged at the higher, 80 g L^{-1} PEG. Plants transferred from 20 to 10 g L^{-1} PEG had the highest WUE_R. We have found that the physiological impedance provides more reliable information of plant water status compared with Ψ_L, which can help improve the irrigation WUE.

1. Introduction

Chinese violet cress (*Orychophragmus violaceus*) of the Brassicaceae family is a horticultural plant species widely planted across China (Wang et al., 2014). This species is a wholesome vegetable that can be eaten year-round, and the plants are also cultivated for medicinal, ornamental and afforestation uses (Kole, 2011). *O. violaceous* is a relatively drought resistant species that is able to grow across the karst regions in limestone soil (Wu and Xu, 2011). It has been also identified as a marginal land-based biomass feedstock (Wang et al., 2014). *O. violaceous* grown in karst areas often suffers from waterlogging and various degrees of drought stress in a short time due to the shallow soil and rapid leakage of surface water (Butscher and Huggenberger, 2009). This makes it difficult to implement appropriate irrigation regimes, especially since agricultural water in karst areas is scarce, especially during winter drought periods. As a result, plant productivity may be severely reduced limiting local economic development (Xing et al., 2019). Therefore, timely and accurate determination of plant water status can help to ensure the optimal water delivery for plant growth and save agricultural irrigation water.

The assessment of plant water status has been often determined based on the leaf appearance, leaf water content, leaf water potential (Ψ_L) measurements, temperature and various growth traits (Luo et al., 2014; Gaudin et al., 2017; Rascio et al., 2020). However, plant water

Abbreviations: CA, carbonic anhydrase; CA_{PEG}, CA activity at each PEG level; CA_{REF}, CA activities at 0 g L^{-1} PEG; C_i, intracellular ion concentration; C_o, extracellular ion concentration; CP, physiological capacitance; E_m, elasticity modulus; F_g, gripping force; g_s, stomatal conductance; LT, leaf tensity; F_s, stresses; LWC, leaf water content; LWC_D, LWC during drought phase; LWC_R, LWC during re-watering phase; LWDR, leaf water dissipation rate; $LWDR_i$, leaf inherent water dissipation rate; M_i, mass of iron; PEG, polyethylene glycol; *m*, mass of the foam board and electrode; P_N, net photosynthetic rate; PPFD, photosynthetic photon flux density; P_{NR}, P_N during re-watering phase; P_{ND}, P_N during drought phase; RCA, relative carbonic anhydrase activity; WUE, water-use efficiency; WUE_i, instantaneous water-use efficiency; WUE_R, re-watering water-use efficiency; Z, impedance; Ψ_L, leaf water potential; ΔX, deformation rates.

* Corresponding author.
E-mail address: wuyanyou@mail.gyig.ac.cn (Y. Wu).

https://doi.org/10.1016/j.scienta.2020.109763
Received 21 June 2020; Received in revised form 2 September 2020; Accepted 23 September 2020
Available online 30 September 2020

status can be affected by the enzymatic activity, including carbonic anhydrase (CA, EC 4.2.1.1), which alters the variation in Ψ_L and reduces the accuracy of diagnosis of water deficit using Ψ_L, leading to a decrease of the irrigation water-use efficiency WUE (Fernández et al., 2015). CA is a zinc-containing enzyme that is widely distributed and involved in diverse physiological processes in animals, plants, archea, and eubacteria by catalyzing the conversion of intracellular bicarbonate into H_2O and CO_2 under drought conditions (Xing and Wu, 2012). Plant water status can also be affected by the elastic properties of cell walls, which play a crucial role in bearing external load (Fila et al., 2019). Fortunately, it is feasible to represent the plant physiological response traits using leaf physical characteristics, which are sensitive to water deficit and can be easily and timely measured (Li et al., 2014).

Electrophysiological properties have been increasingly used for diagnosing plant water status since the variation of plant cell volume and cell sap concentration are closely correlated with electrophysiological indexes such as physiological capacitance (CP), impedance (Z), resistance or leaf tensity (LT) (Jócsák et al., 2019; Zhang et al., 2015b). These indices can be determined with a nondestructive custom-made parallel-plate capacitor which employs a given frequency and voltage. The physiological capacitance (CP) and Ψ_L are related to the cell sap concentration. Leaf CP is associated with the effective thickness and area of leaves in contact with capacitor plates. The ratio of leaf area and leaf effective thickness is defined as LT (Zhang et al., 2015b). However, the cytosol solute concentration as well as the elasticity and plasticity of leaf cells are highly responsive to the variable gripping forces (F_g), which are used for clamping a leaf during the measurement (Zhang et al., 2015b). The index that is determined using a specific gripping force is an instantaneous value that can only represent an instantaneous water status. There is a positive correlation between tissue internal architecture and water loss (Cruz et al., 2019). The inherent tissue water status has been investigated by analyzing the mechanical properties which are closely related to leaf internal architectures (Balsamo et al., 2015). However, plant tissues are irreversibly damaged during the measurements of mechanical properties by compressing the leaf with a failure load.

Plant cells are composed of protoplasts and cell walls. The vacuoles and cytoplasm, which are the main electrolytic inclusions in the protoplasts, are surrounded by the tonoplast and plasma membrane, respectively. Cytoplasm contains numerous organelles with specific membranes, and the vacuole contains mainly dissolved inorganic ions and organic acids (Zhang et al., 2015a). Electric potential difference is produced when current passes the cell membrane, and it is retained by the efficient transport system and the alternative permeability of the cell membrane (Lindén et al., 2016). Electrical characteristics vary between the organelles, the vacuole and the cytoplasm, which occupy most of the space in cells and can be regarded as resistors, while the plasma membrane has a capacitive characteristic. When alternating current flows through the plant tissue, the ratio of the passing current between the extracellular and intracellular spaces is influenced by the frequency of the alternating current and tissue features. Electric current is always affected by the resistors, capacitors and inductors in the alternating current circuit, and impedance is the sum of the resistance to current caused by the resistors, capacitors and inductors (Schönleber and Ivers-Tiffée, 2015). The mesophyll cell can be regarded as a concentric sphere capacitor with both inductor and resistor functions. Nevertheless, when the electrical impedance characteristics of a plant are characterized and used to represent the leaf water status, inductors are not the actual parts of the circuit models derived from plant leaves and are not involved in the movement of water into and out of cells. However, plant leaf water status and cell internal architecture are still correlated with cell impedance characteristics, which can provide more reliable information of the plant water status than leaf water potential.

Here we aimed at determining the variation of impedance induced by the increasing external gripping forces which were far lower than the force of failure load, to investigate the leaf water status under osmotic stress and subsequent drought hardening, to provide basis for further research on the accurate monitoring of plant water status. Based on the understanding of leaf water status, the drought hardening effect could be assessed more exactly by using re-watering water-use efficiency (WUE_R) rather than the instantaneous water-use efficiency (WUE_i), the latter one was determined by the LI-6400XT photosynthesis measurement system. WUE_R is the increment of net photosynthetic rate (P_N) per increment of leaf water content (LWC) in leaves from drought to re-watering phase, which gives the plants sufficient time to regulate and balance water supply (Javed et al., 2018).

Polyethylene glycol molecules with a molecular weight $\geq$ 6000 (PEG 6000) are inert, non-ionic and cell impermeable. They are small enough to influence the osmotic pressure, but large enough unabsorbed by plants (Xing and Wu, 2012). Therefore, they were used to simulate osmotic stress in this study. The seedlings of *O. violaceous* were selected and grown during the winter drought period and subjected to osmotic stress induced by PEG 6000 and following drought hardening to study the responses of LWC, Ψ_L, CA activity, photosynthetic characteristics, leaf electrophysiological and mechanical properties, and WUE_R.

2. Materials and methods

2.1. Plant growth and treatment

The research was carried out in a growth chamber at the Institute of Agricultural Engineering, Jiangsu University, Jiangsu Province, China (N 32°11′ and E 119°27′). The seedlings of *O. violaceous* were germinated and cultivated in 12 drain-cavity-containing plastic trays layered with quartz sand under a 12 h photoperiod (260 ± 20 μmol m^{-2} s^{-1} PPFD), day/night temperature cycle of 28 °C/20 °C and 65 ± 5% relative humidity (He et al., 2010). The size of each cavity was 4 × 4 × 5.5 cm (length × width × depth), the size of the tray base was 19 × 14 × 6.5 cm. 250 mL 1/2-strength Hoagland solution was added into each tray at the beginning, and the solution was changed with a new batch of 250 mL 1/2-strength Hoagland solution everyday (Xing et al., 2016). The Hoagland's solution contains 6 mM KNO_3, 4 mM $Ca(NO_3)_2$, 2 mM $MgSO_4$, 2 mM FeEDTA, 1 mM $NH_4H_2PO_4$, 2 μM KCl, 50 μM H_3BO_3, 4 μM $MnSO_4$, 4 μM $ZnSO_4$, 0.2 μM $CuSO_4$, and 0.2 μM $(NH_4)_6MO_7O_{24}$. After 45 days of growth, the 1/2-strength Hoagland solution was replaced by treatment solution (polyethylene glycol (PEG) 6000 dissolved in Hoagland solution). Five osmotic stress levels were applied to induce water deficit stress by adding PEG 6000 (0, 10, 20, 40, and 80 g L^{-1}) into Hoagland solution. Twenty-four seedlings that germinated healthily and uniformly in every two trays were used for each stress level. The hydroponic solution without PEG was intended to simulate slight waterlogging stress according to the results in our previous research, which demonstrated that *O. violaceous* maintained higher water status at 10 g L^{-1} PEG (Xing et al., 2016). The variations of leaf electrophysiological and mechanical properties under different degrees of osmotic stresses were stimulated and determined. The 10 g L^{-1} PEG treatment was used as a control. In addition, the plants grown in 0 g L^{-1} PEG solution were cultured continuously in the 0 g L^{-1} PEG solution during the drought hardening phase as another primary control group. The drought resistance was induced by transferring the plants into lower PEG 6000 concentration level to investigate the leaf water status and recovery of cell elasticity. The drought hardening treatment was imposed on day eight following the onset of the osmotic stress treatment. During the drought hardening phase, the five different treatment solutions which were used to irrigated the seedlings in the 0, 10, 20, 40, and 80 g L^{-1} PEG treatment levels were replaced by the treatment solutions which contained 0, 0, 10, 20, and 40 g L^{-1} PEG, respectively. The drought hardening treatment phase lasted 4 days. The solution was changed with a new batch of mixed solution every other day during the treatments. Measurements were conducted on day eight after the onset of the osmotic stress treatment and day four after the onset of the drought hardening treatment. The fourth and fifth youngest fully

expanded leaves from the top (five plants from each treatment group) were chosen for measurements.

2.2. Determination of leaf water content, water potential and leaf tensity

The CP was measured using an LCR tester (*Model 3532-50, Hioki*, Nagano, Japan), the frequency and voltage used were 3 KHz and 1 V, respectively. With a dew point microvoltmeter in a universal sample room (C-52-SF, Psypro, Wescor, Logan, Utah), Ψ_L was measured at the same position of the leaves with the above CP testing. The leaf tensity (LT, $cm^2\,cm^{-1}$) of leaves at each stress level was calculated according to Zhang et al. (2015b). The leaves were dried in an oven at 80 °C. The fresh (W_F) and dry weights (W_D) were determined using an electronic analytical balance (*BSA124S*, *Sartorius*, Gottingen, Germany). Leaf water content (LWC) was calculated as $LWC = \frac{W_F - W_D}{W_F} \times 100\%$.

2.3. Determination of physiological capacitance and impedance at different gripping forces

The variation of CP and Z as increased gripping forces were determined using the LCR tester with a frequency and voltage of 3 KHz and 1 V, respectively. Each leaf was clipped onto the custom-made parallel-plate capacitor (Fig. 1).

2.4. Calculation of leaf water dissipation rate based on impedance

The following equation was used to calculate gripping forces (F_g, N), which were used for clamping a leaf during the CP and Z measurements:

$$F_g = (M_i + m)g \tag{1}$$

where F_g is the gravity (gripping force, N); M_i is the mass of iron (kg); m is the mass of the foam board and electrode (kg); and g is the acceleration of gravity with a value of 9.80 N kg^{-1}.

Electrophysiological behavior of a plant is closely related to that of a single cell, and the cell can be presumed as a spherical capacitor. Cell impedance mainly depends on the ratio of ion concentrations between the intramembrane and extramembrane space when the measurement is conducted within a single object in the same situation. Therefore, leaf impedance values change with the changing cell water content and cell membrane permeability. The latter can be influenced by the external stimulus, which changes the ion concentrations inside and outside of the membrane. The Nernst equation can be applied to the difference of the ion concentrations mentioned above, and impedance is inversely proportional to intracellular ion concentration at a given extracellular ion concentration. As such, the relationship between impedance and external stimulus can be derived.

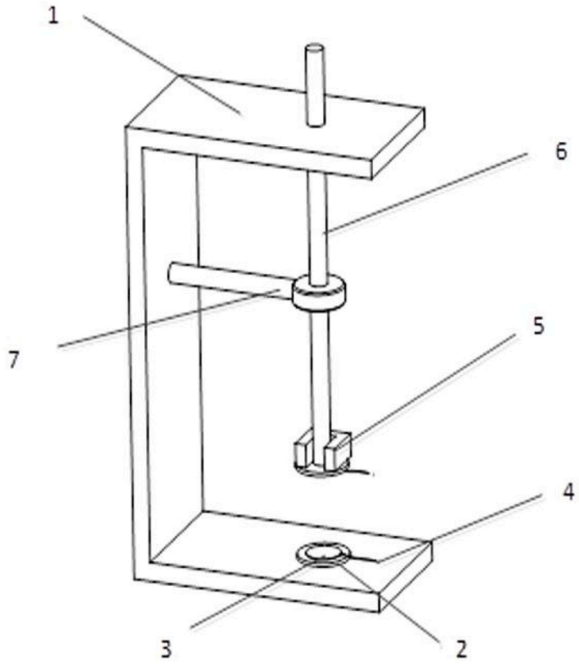

Fig. 1. Schematic of the parallel-plate capacitor: 1= bracket; 2= foam board; 3= electrode; 4= wire; 5= iron; 6= plastic bar; 7= fixation clamp.

Cell elasticity in leaves is correlated to water status, changes in permeability of cell membrane differ with plants at a given gripping force, and the impedance differs between different plants.

The Nernst equation is:

$$E - E^0 = \frac{RT}{nF_0}\ln\frac{C_i}{C_o} \tag{2}$$

where E is the electromotive force (V); E° is the standard electromotive force (V); R is the gas constant (8.31 J K^{-1} mol^{-1}); T is the thermodynamic temperature (K); C_i is the intracellular ion concentration (mol L^{-1}); C_o is the extracellular ion concentration (mol L^{-1}); F_0 is the faraday constant (9.65×10^4 C mol^{-1}); n is the ion transfer amount (mol).

The work produced is due to pressure which is transformed from the internal energy of electromotive force, and it displays a positive correlation with PV (PV = aE). Thus,

$$PV = aE = aE^0 + \frac{aRT}{nF_0}\ln\frac{C_i}{C_o} \tag{3}$$

where P is the pressure imposed on leaf cells, Pa; "a" is the transfer coefficient form electromotive force to energy; V is the cell volume, m^3; P is calculated as: $P = \frac{F_g}{S}$, where F_g is the gripping force; S is the effective area of leaf that is in contact with capacitor plants, m^2.

Vacuole and cytoplasm occupy most of the space in the developed mesophyll cells. In terms of the mesophyll cell, the sum of C_o and C_i is constant, which is equal to the total ion concentration inside and outside of the membrane. C_i is positively correlated to electrical conductivity, and the electrical conductivity is the reciprocal of Z. Therefore, $\frac{C_i}{C_o}$ can be expressed as $\frac{C_i}{C_o} = \frac{\frac{f}{Z}}{C-\frac{f}{Z}} = \frac{f}{CZ-f}$, where f is the transfer coefficient between C_i and Z. The Eq. (3) can be rewritten as follows:

$$\frac{V}{S}F_g = aE^0 - \frac{aRT}{nF_0}\ln\frac{CZ-f}{f} \tag{4}$$

Then

$$\ln\frac{CZ-f}{f} = \frac{nF_0E^0}{RT} - \frac{VnF_0}{SaRT}F_g \tag{5}$$

The logarithmic Eq. (5) written in base *e* can be solved as follows:

$$\frac{CZ-f}{f} = e^{\frac{nF_0E^0}{RT}}e^{\left(-\frac{VnF_0}{SaRT}F_g\right)} \tag{6}$$

The impedance can be calculated as follows:

$$Z = \frac{f}{C} + \frac{f}{C}e^{\frac{nF_0E^0}{RT}}e^{\left(-\frac{VnF_0}{SaRT}F_g\right)} \tag{7}$$

where Z is the impedance, MΩ.

In terms of a single leaf in the same situation, V, S, a, E^0, R, T, n, F_0, C and f are constants, incorporating $y_0 = \frac{f}{C}$, $k = \frac{f}{C}e^{\frac{nF_0E^0}{RT}}$ and $b = \frac{VnF_0}{SaRT}$ into Eq. (7) changes this equation to:

$$Z = y_0 + ke^{-bF_g} \tag{8}$$

where y_0, k and b are the model parameters.

The derivative of Eq. (8) is as follows:

$$Z' = -bke^{-bF_g} \tag{9}$$

Leaf physiological impedance represents the resistance to current, which is generated by the transport of dielectric materials including inorganic and organic ions. Leaf water dissipation rate (LWDR) is negatively correlated with the value of Z'. Therefore, LWDR at a given gripping force can be expressed as LWDR $= -Z'$.

2.5. Measurement of leaf elasticity modulus

The increased stresses (F_s, N) with increasing deformation rates (ΔX, %) of leaf at each osmotic stress level and following stress relief were recorded with the texture analyzer TA.XT-Plus (Stable Micro System, United Kingdom) using the P/2n probe with a diameter of 2 mm. The instrument working parameters were determined by the test mode compression; with pretest speed at 2 mm s^{-1}, test speed at 1 mm s^{-1}, post-test speed at 2 mm s^{-1}. The leaf elasticity modulus (E_m, N per unit deformation) was then calculated according to Eq. (10) as follows:

$$F_s = E_m \times \Delta X \quad (10)$$

2.6. Measurement of carbonic anhydrase activity and photosynthetic parameters

Carbonic anhydrase activity was determined with the electrometrical method of Wilbur and Anderson (1948) with modifications (Wu et al., 2011). The relative value of CA activity obtained at each treatment level was calculated using RCA $= \frac{CA_{PEG}}{CA_{REF}}$, where CA_{PEG} represented the CA activity at each PEG level, and the CA activities at 0 g L^{-1} PEG during osmotic stress and following stress relief phases were taken as CA_{REF}, respectively. The photosynthetic parameters were measured and calculated according to Xing and Wu (2012).

2.7. Calculation of re-watering water-use efficiency

The WUE_R was calculated according to the method described by Javed et al. (2018).

$$WUE_R = \frac{P_{NR} - P_{ND}}{LWC_R - LWC_D} \quad (11)$$

Where P_{NR} and LWC_R is the P_N and LWC during drought hardening phase; P_{ND} and LWC_D is the P_N and LWC during stress phase; WUE_R is the re-watering water-use efficiency, mmol (CO_2) mol^{-1} (H_2O).

2.8. Statistical analysis

Data were analyzed using exploratory data analysis by SPSS software (version 13.0, SPSS Inc.). Statistically significant differences between stress levels were assessed using the least significant difference (LSD) post-hoc test at the 5% significance level ($p \leq 0.05$). The data are shown as the means ± SE, which were determined using one-sample t test (confidence interval was 95 %, $n = 5$).

3. Results

3.1. Leaf water content, water potential and leaf tensity

The values of LWC at 40 and 80 g L^{-1} PEG treatments sharply decreased compared to those at 0, 10 and 20 g L^{-1} treatments during the phase of osmotic stress (Fig. 2a). The values of LWC for 40 and 80 g L^{-1} treatments were still greatly lower compared with those in 0 and 10 g L^{-1} treatments during the drought hardening phase. The LWC values in each treatment level increased after drought hardening compared to those in the osmotic stress phase. The highest Ψ_L value was observed in the 10 g L^{-1} PEG treatment during the stress phase (Fig. 2b). The Ψ_L values decreased with the osmotic stress level. For the drought hardening phase, there was little difference between the Ψ_L values at the levels ranging from 0 to 40 g L^{-1}, while the Ψ_L value in the 80 g L^{-1} remained relatively low (Fig. 2b). In the control (0 g L^{-1} PEG treatment), LT was the highest during the stress phase, and it decreased with increasing stress level (Fig. 2c). However, there was no significant difference between the LT values in PEG treatment concentration levels ranging from 20 to 80 g L^{-1}. LT in the 0 g L^{-1} (control) was also the highest during the drought hardening phase, and there was no significant difference between those values in treatment levels ranging from 10 to 80 g L^{-1}.

3.2. Effect of gripping force on physiological capacitance in each treatment during stress and drought hardening phases

The results of CP variation determined by compressing the leaves with different external gripping forces are shown in Fig. 3. Low CP values were associated with high PEG treatment concentrations with the exception of the 20 g L^{-1} PEG treatment (Fig. 3a). The CP values displayed a positive correlation with gripping forces at each PEG level during the stress phase (Fig. 3a). However, the value of CP in the 20→10 g L^{-1} treatment was not always clearly different from that in the 40→20 g L^{-1} treatment even under the same gripping force during the drought hardening phase (Fig. 3b).

3.3. Leaf water dissipation rate and elasticity modulus

The relationship curves between Z and F_g for *O. violaceus* at different PEG levels were established using SigmaPlot (ver. 12.5, Systat Software, Inc., San Jose, Cal.) (Fig. 4). The relationships between Z and F_g were fitted. The model parameters y_0, k and b were estimated, respectively (Table 1). According to Eq. (9), the value of LWDR was defined as leaf inherent water dissipation rate ($LWDR_i$) when F_g equaled zero.

The values of $LWDR_i$ in the 20 and 40 g L^{-1} PEG treatments were significantly higher than those in the 0, 10 and 80 g L^{-1} PEG treatments and there was no significant difference between the $LWDR_i$ values in the 0, 10 and 80 g L^{-1} PEG treatments during the stress phase. While the values of $LWDR_i$ at 10 g L^{-1} treatment was significantly higher

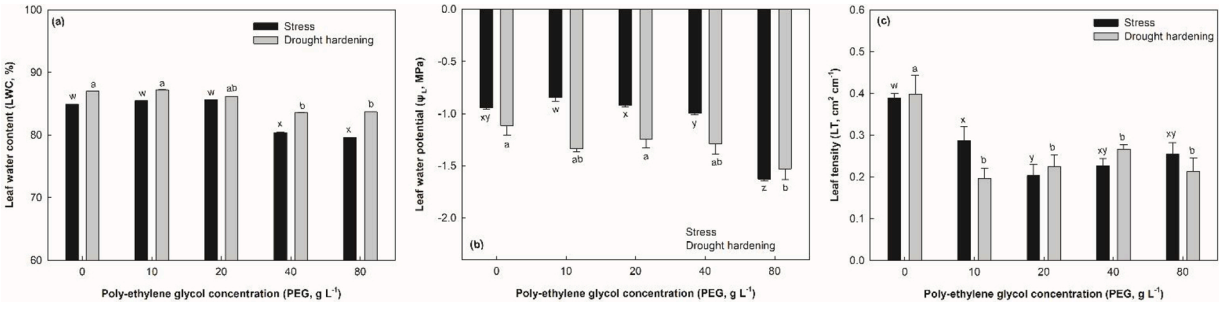

Fig. 2. Leaf water content (LWC, %), water potential (Ψ_L, MPa) and leaf tensity (LT cm^2 cm^{-1}) of *O. violaceus* during the stress and drought hardening phases (Note: (a) LWC; (b) Ψ_L; (c) LT. The means ± SE ($n = 5$) followed by different letters in the same treatment phase in each index differ significantly at $P \leq 0.05$, according to one-way ANOVA and t test. (w, x, y et al.) indicate the difference of the values in the stress phase and (a, b, c et al.) indicate those in drought hardening phase).

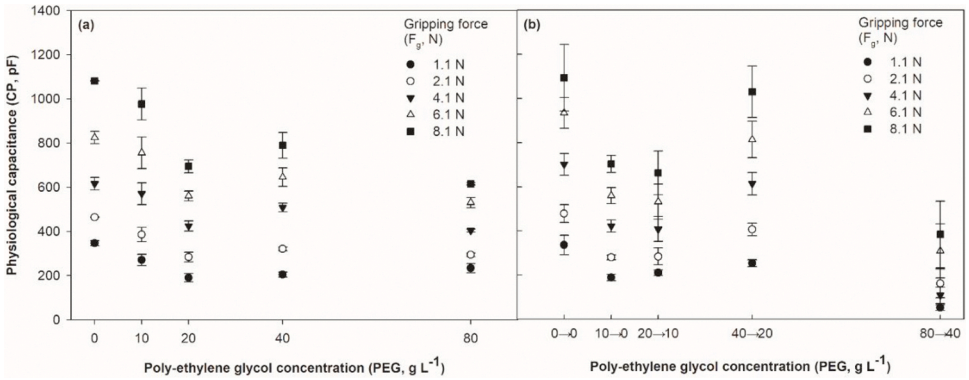

Fig. 3. Effect of gripping force (F_g, N) on leaf physiological capacitance (CP, pF) of *O. violaceus* in each treatment during the stress (a) and drought hardening (b) phases. (Note: → represents drought hardening treatments in which plants were transferred from higher to lower PEG concentrations).

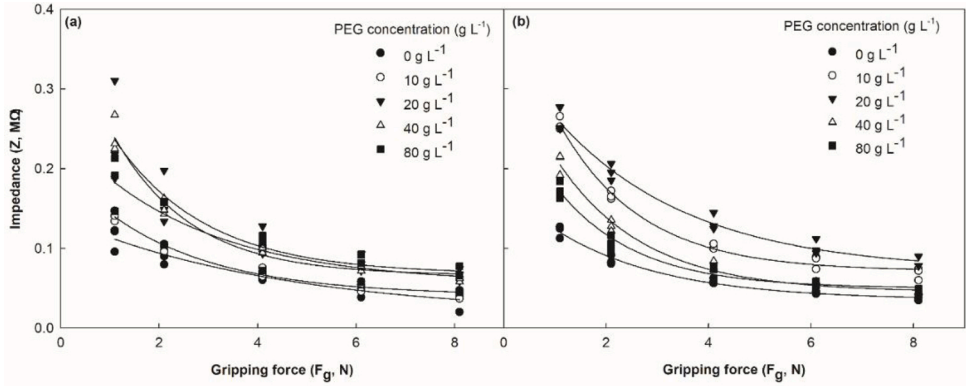

Fig. 4. The relationship curves between impedance (Z, MΩ) and gripping force (F_g, N) for *O. violaceus* at different PEG concentrations (g L^{-1}) during the stress (a) and drought hardening (b) phases.

Table 1
Fitting equations of the relationship between impedance (Z, MΩ) and gripping force (F_g, N).

Treatment period	PEG concentration (g L^{-1})	Fitting equations	R^2	n	P
Stress phase	0	$Z = 0.015 + 0.123e^{-0.223F_g}$	0.9098	15	<0.0001
	10	$Z = 0.041 + 0.162e^{-0.446F_g}$	0.9794	15	<0.0001
	20	$Z = 0.068 + 0.303e^{-0.534F_g}$	0.8315	15	<0.0001
	40	$Z = 0.066 + 0.348e^{-0.633F_g}$	0.9725	15	<0.0001
	80	$Z = 0.056 + 0.191e^{-0.372F_g}$	0.8178	15	<0.0001
Drought hardening phase	0→0	$Z = 0.035 + 0.142e^{-0.466F_g}$	0.9793	15	<0.0001
	10→0	$Z = 0.071 + 0.365e^{-0.625F_g}$	0.9909	15	<0.0001
	20→10	$Z = 0.071 + 0.284e^{-0.381F_g}$	0.9806	15	<0.0001
	40→20	$Z = 0.045 + 0.307e^{-0.590F_g}$	0.9856	15	<0.0001
	80→40	$Z = 0.050 + 0.247e^{-0.647F_g}$	0.9754	15	<0.0001

Note: → represents drought hardening treatments in which plants were transferred from higher to lower PEG concentrations.

compared to 0 and 20 g L^{-1} treatments, those in the 0, 20, 40 and 80 g L^{-1} treatments showed no significant difference during the drought hardening phase. A significant increase in E_m of plants was observed at 40 g L^{-1} during the stress phase (Fig. 5). Higher values of E_m were associated with higher PEG treatment concentrations between the levels ranging from 20 to 80 g L^{-1}, and the values of E_m in the 0, 10 and 20 g L^{-1} PEG treatments exhibited no significant differences during the drought hardening phase.

3.4. Carbonic anhydrase activity and net photosynthesis rates

During the stress phase, CA activity was the lowest in plants subjected to the 10 g L^{-1} PEG treatment and the highest in plants exposed to 40 g L^{-1} PEG (Fig. 6a). CA activity in the 20 g L^{-1} treatment was lower than that in control plants (0 g L^{-1} PEG). During the drought hardening phase, the CA activity was the highest in plants treated with 10 g L^{-1} PEG and decreased with increasing PEG stress between the levels ranging from 10 to 80 g L^{-1} PEG. P_N was significantly lower in the 40 and 80 g L^{-1} treatments compared to those in the 0 and 10 g L^{-1} PEG during the stress phase, while the P_N in 0, 10 and 20 g L^{-1} treatments increased after drought hardening compared to at the stress phase (Fig. 6b). The values of g_s sharply decreased in the 20 g L^{-1} and higher PEG concentration treatments during the stress phase (Fig. 6c). In the 10, 20 and 40 g L^{-1} PEG treatments, g_s were slightly lower during drought hardening compared with the stress phase (Fig. 6c).

3.5. Correlation of parameters

The Pearson correlation coefficients for the relationship of Ψ_L, LWC, CP, LT, $LWDR_i$, E_m and P_N are shown in Table 2. P_N was significantly

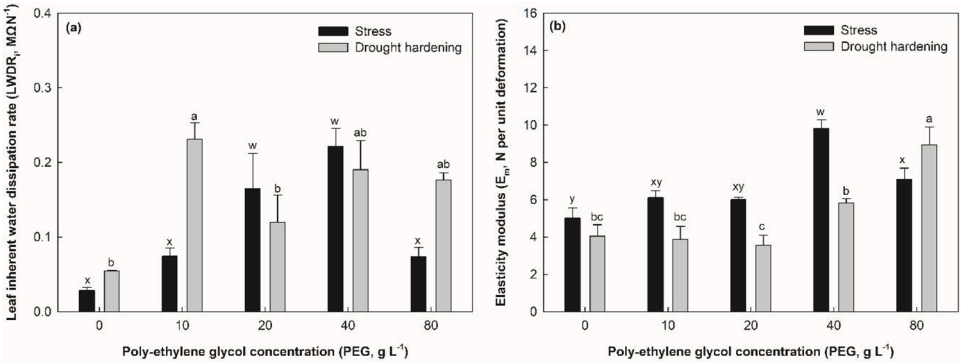

Fig. 5. Leaf inherent water dissipation rate ($LWDR_i$, MΩ N^{-1}) and elasticity modulus (E_m, N per unit deformation) of *O. violaceus* during the stress and drought hardening phases (Note: (a) $LWDR_i$; (b) E_m. The means ± SE (n = 5) followed by different letters in the same treatment phase in each index differ significantly at $P \leq 0.05$, according to one-way ANOVA and t test. (w, x, y et al.) indicate the difference of the values in the stress phase and (a, b, c et al.) indicate those in drought hardening phase).

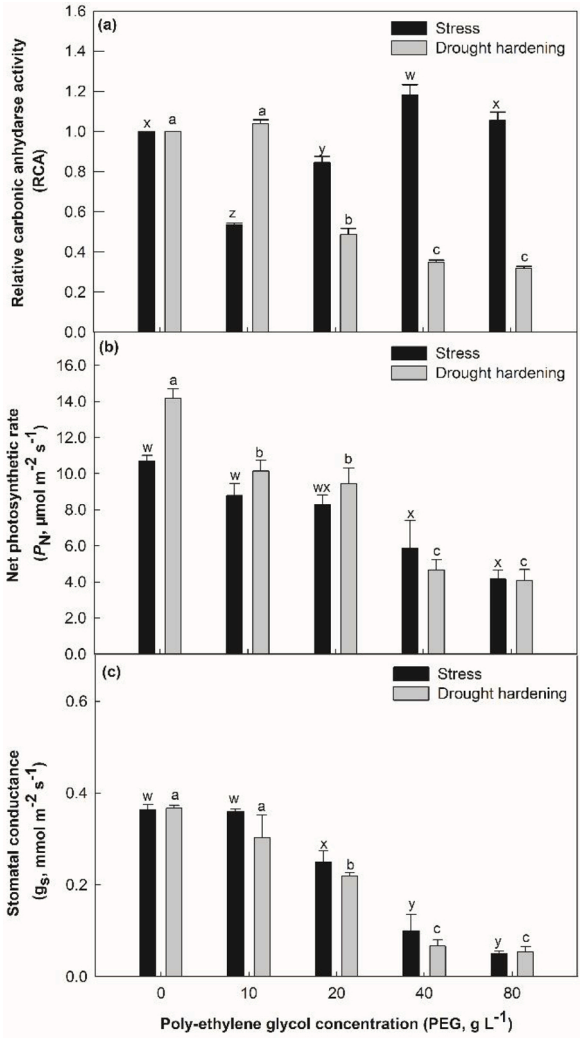

Fig. 6. The relative carbonic anhydrase activity (RCA), net photosynthetic rate (P_N, μmol m^{-2} s^{-1}) and stomatal conductance (g_s, mmol m^{-2} s^{-1}) of *O. violaceus* during the stress and drought hardening phases (Note: (a) RCA; (b) P_N; (c) g_s. The means ± SE (n = 5) followed by different letters in the same treatment phase in each index differ significantly at $P \leq 0.05$, according to one-way ANOVA and t test. (w, x, y et al.) indicate the difference of the values in the stress phase and (a, b, c et al.) indicate those in drought hardening phase).

correlated with LWC, CP, LT and E_m. $LWDR_i$ and E_m were significantly correlated with LT and LWC, respectively. However, Ψ_L exhibited no significant relationship with LWC, LT, $LWDR_i$ and E_m.

Table 2
Correlation of leaf water potential (Ψ_L, MPa), water content (LWC, %), physiological capacitance (CP, pF), leaf tensity (LT, cm^2 cm^{-1}), leaf inherent water dissipation rate ($LWDR_i$, MΩ N^{-1}), elasticity modulus (E_m, N per unit deformation) and net photosynthetic rate (P_N, μmol m^{-2} s^{-1}) (n = *30*).

	LWC	CP	LT	$LWDR_i$	E_m	P_N
Ψ_L	0.29	0.36*	0.24	−0.17	−0.08	0.46*
LWC		0.20	0.17	−0.10	−0.66**	0.73**
CP			0.99**	−0.66**	−0.36	0.51**
LT				−0.66**	−0.36*	0.47**
$LWDR_i$					0.28	−0.40*
E_m						−0.61**

* Correlation is significant at the 0.05 level (2-tailed).
** Correlation is significant at the 0.01 level (2-tailed).

3.6. *Instantaneous water-use efficiency and re-watering water-use efficiency*

The value of WUE_i sharply increased in the 80 g L^{-1} treatment during the stress phase. The values of WUE_i at each PEG concentration level increased during drought hardening compared to the stress phase (Table 3). The WUE_R of plants subjected to the 20 g L^{-1} PEG treatment was the highest during drought hardening, and the value of WUE_R in control (0 g L^{-1} PEG) plants was higher compared with plants treated with 10 g L^{-1} PEG (Table 3). The WUE_R in the 20 g L^{-1} treatment was almost twice as high compared with 0 g L^{-1} control.

4. Discussion

4.1. *Leaf water potential, leaf tensity and variation of physiological capacitance*

Water potential is commonly used to assess plant water status, Ψ_L is usually closely related to the leaf net photosynthesis (Santesteban et al., 2019). However, in our study, the significant decrease of LWC and P_N

Table 3
Instantaneous water-use efficiency (WUE_i, mmol (CO_2) mol^{-1} (H_2O)) and re-watering water-use efficiency (WUE_R, mmol (CO_2) mol^{-1} (H_2O)) in *O. violaceus* plants subjected to PEG stress and following drought hardening.

PEG concentration (g L^{-1})	WUE_i (mmol (CO_2) mol^{-1} (H_2O))		WUE_R (mmol (CO_2) mol^{-1} (H_2O))
	Stress	Drought hardening	
0	2.70 ± 0.13b	4.48 ± 0.15a	582.80
10	2.08 ± 0.11b	3.74 ± 0.10b	449.09
20	2.23 ± 0.22b	3.94 ± 0.23a	1146.69
40	2.92 ± 0.16ab	4.96 ± 0.06a	–415.05
80	3.62 ± 0.04a	5.13 ± 0.70a	–24.82

Note: The mean ± SE (n = 5) followed by different letters in the same column differ significantly at $P \leq 0.05$, according to one-way ANOVA and t test.

was inconsistent with that of Ψ_L. *O. violaceus* is a drought-resistant species, but may not tolerate well the slight waterlogging stress in this culture system. We previously demonstrated that this effect could be alleviated by the addition of PEG (Xing et al., 2016). The seedlings maintained higher water status at 10 g L^{-1} PEG treatment than that at 0 g L^{-1} PEG, and 10 g L^{-1} PEG treatment could be used as a control. The alleviation of waterlogging stress in plants by the 10 g L^{-1} PEG treatment was likely the factor contributing to an increase in Ψ_L compared to that at 0 g L^{-1} PEG. As such, CA activity exhibited a relative low value in the 10 g L^{-1} treatment because plants did not suffer from severe water deficit and the photosynthesis at this level was not inhibited. The increased CA activities in the 20 and 40 g L^{-1} treatments could efficiently promote the conversion of intracellular HCO_3^- to H_2O, which prevented Ψ_L from decreasing, but only the P_N in the 20 g L^{-1} rather than 40 g L^{-1} treatment exhibited no significant decrease compared with that in the 10 g L^{-1} treatment. When the plants were transferred form 10 and 20 g L^{-1} PEG treatments to 0 and 10 g L^{-1} PEG treatments, respectively. The values of Ψ_L during the drought hardening phase decreased compared to at the stress phase, while the values of P_N increased. Therefore, it was not appropriate to determine the water deficit status of *O. violaceous* with just Ψ_L. Calculated according to the coupling relationship between Ψ_L and CP, LT reflects water status better than Ψ_L (Zhang et al., 2015b). Slight decrease in P_N at 20 g L^{-1} compared to 10 g L^{-1} was associated with a decrease in LT during the stress phase. However, the decrease in P_N during the whole treatment period was not always correlated with the variation of LT. CP values changed as the gripping force and PEG concentration changed. Leaf effective thickness was also affected by the water deficit stress, the gripping force would be influenced when the measurement was conducted on these leaves. The observed differences between values of CP or LT could be mainly due to the significant variation of leaf effective thickness rather than the imposed gripping force itself. As an instantaneous value at a specific gripping force, CP or the correspondingly calculated value of LT could not always represent the plant water status correctly. For instance, it would be uncertain whether there was a difference between CP values in the 20 and 40 g L^{-1} PEG treatments without an appropriate uniform gripping force for the electrophysiological index determination.

4.2. Leaf water dissipation rate and elasticity modulus

The above drawbacks can be avoided by determining the variation rate of the electrophysiological index at increasing gripping forces. The variation of physiological impedance is correlated to the cytosol solute concentration and cell elasticity in leaves, and it represents the intracellular water or dielectric materials variation traits (Garcia-Navarro et al., 2019). In this study, the physiological impedance was determined by compressing the leaf with a series of different gripping forces. The coupling model between gripping force and physiological impedance was established according to the Nernst equation. Leaf water dissipation rate (LWDR) based on the physiological impedance was calculated by taking the derivative of the above-mentioned coupling model.

Stomatal control is a major physiological factor to optimize the use of water under water deficit conditions (Vaziriyeganeh et al., 2018). *O. violaceous* plants treated with 10 g L^{-1} PEG showed a slight stomatal closure but a clear increase in $LWDR_i$ after drought hardening. Similarly to Guo et al. (2017), leaf cell elasticity of *O. violaceous* at 10 g L^{-1} PEG increased due to the improved water status following drought hardening, while cell stiffness concomitantly decreased. As a result, the photosynthetic capacity of plants was promoted. On the other hand, during the photosynthetic process, the water and CO_2 supply was not reduced by the slight stomatal closure after transferring plants from 10 to 0 g L^{-1} PEG, which could be responsible for upregulation of CA activity in leaves. The significant decrease of Ψ_L in plants transferred from 10 to 0 g L^{-1} PEG was due to the negative pressure, which could be caused by a short-term fast increase of cell elasticity, water consumption during the photosynthesis process or the increase of water dissipation rate in cells (Fig. 7).

Compared to the $LWDR_i$ in the 10 g L^{-1} PEG treatment, the increase in $LWDR_i$ in the 20 g L^{-1} treatment did not reduce the cell elasticity, which likely explained the similar values of E_m between 10 and 20 g L^{-1} treatments. However, the remarkable water loss caused a significant decrease in Ψ_L and reduced LT in the 20 g L^{-1} treatment. Seedlings in this treatment showed a clear decrease in g_s, the intracellular water could then be efficiently used to maintain the photosynthesis. After drought hardening, cell elasticity increased due to the improved water status, which decreased the E_m but reduced the Ψ_L. Further decrease of g_s prevented the continuous water loss in the 40 g L^{-1} PEG level, while Ψ_L and cell elasticity decreased due to the limited water supply and almost the same water dissipation rate with that in the 20 g L^{-1} treatment, water deficit inhibited photosynthesis in the 40 g L^{-1} PEG level. The highest activity of CA at this level played an important role in regulating the intracellular water balance, which maintained the LT. After drought hardening, the improved water status increased the cell elasticity, and E_m decreased. However, photosynthetic recovery was not observed. The short-term fast increase of cell elasticity reduced the Ψ_L, but photosynthesis was still inhibited at 40 g L^{-1} treatment due to the reduction of intracellular water. The serious damage to cells and photosynthesis in plants occurred in the 80 g L^{-1} PEG treatment and an obvious water and solute leakage would be expected to happen which was implied by the significant decrease in $LWDR_i$ and the unrecoverable cell elasticity from the stress to drought hardening phase at 80 g L^{-1} treatment.

4.3. Leaf water dissipation rate and water-use efficiency

Under drought conditions, leaf cells respond to water deficit by changing the cell elasticity and sap concentration, to improve the water-use efficiency (WUE) and adjust to stress (Bian et al., 2016). In this study, it was observed that WUE_i was not directly correlated with stomatal movement or water dissipation rate, and it would not be a suitable parameter for evaluating the effect of drought hardening in *O. violaceus*. WUE_R is a relatively recent technique used to determine the water status of the plant leaf and the impact of water status on photosynthetic activities, and it has been successfully used for optimizing the re-watering

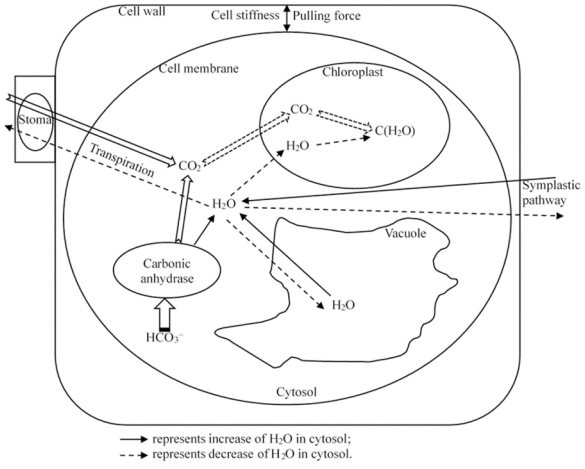

Fig. 7. Water status in leaf cells (Note: Decreases in cell elasticity and leaf water potential (Ψ_L) reduce the leaf tensity (LT) under osmotic stress, but increase the cell stiffness which is represented by leaf elasticity modulus (E_m). Increasing leaf water dissipation rate (LWDR) represents an improved water status which benefits the photosynthesis. Water in cytosol can come from the vacuole or conversion of intracellular HCO_3^- catalyzed by CA, which alters the Ψ_L and LT. After drought hardening, improved water status increases the cell elasticity and decreases the cell stiffness. Increase in LWDR and stomatal closure help to sustain the photosynthesis, water consumption during the photosynthetic process and the water dissipation rate cause a decrease in Ψ_L).

strategy for okra (Azeem et al., 2017). During the stress phase, the stomatal closure of *O. violaceous* at 20 g L^{-1} treatment saved intracellular water and maintained the water for photosynthetic process. Compared to the other drought hardening strategies, plants transferred from 20 to 10 g L^{-1} PEG exhibited better control of water use. The improved water status increased the cell elasticity in plants subjected to this treatment during the drought hardening phase, and promoted the photosynthetic process without extra water dissipation and the supplemental water was efficiently utilized. Therefore, the plants transferred from 20 to 10 g L^{-1} PEG had the highest value of WUE_R. The photosynthetic capacity in plants subjected to the 40 and 80 g L^{-1} PEG treatments was likely too severely affected to recover following drought hardening and the WUE_R values became negative. As such, it was advantageous to transfer the plants treated with 20 g L^{-1} PEG first to 10 g L^{-1} PEG for drought hardening.

In conclusion, the diagnosis of plant water status using Ψ_L, CP or LT at a specific gripping force was not always accurate due to the water regulation in plants or the variation of leaf effective thickness. The LWDR was calculated according to the variation of physiological impedance and provided more reliable information of the plant water status compared with Ψ_L or CP. The intracellular water status can be investigated based on the determination of $LWDR_i$ and E_m. The results of the present study demonstrate that the LWDR altered the intracellular water status, which played an important role in the WUE_R, and WUE_R may be a good parameter for clarifying appropriate drought hardening strategies for *O. violaceous* and deficit irrigation scheduling could be implemented during the winter drought period.

5. Conclusions

The coupling model between gripping force and physiological impedance was established according to the Nernst equation, and the leaf water dissipation rate was defined and determined in this research. This method provided more reliable information of the plant water status compared with Ψ_L or CP. The changes of cell stiffness and leaf water dissipation rate altered the water status in leaf cells, which played an important role in the photosynthesis and re-watering water-use efficiency. Monitoring the water status in plants using physiological impedance is nondestructive and can timely determine the plant water needs, this information could provide support for the improvement of irrigation techniques.

CRediT authorship contribution statement

Deke Xing: Data curation, Writing - original draft. **Lu Chen:** Investigation. **Yanyou Wu:** Funding acquisition, Conceptualization. **Janusz J. Zwiazek:** Writing - review & editing.

Declaration of Competing Interest

The authors reported no declarations of interest.

Acknowledgements

This study was supported by the project of the National Key Research and Development Program of China [2016YFC0502602], the National Natural Science Foundation of China [No. U1612441], the fund of the “Outstanding Young and Middle-Aged University Teachers and Presidents Training Abroad Project” of Jiangsu Province, the Priority Academic Program Development (PAPD) of Jiangsu Higher Education Institutions.

Appendix A. Supplementary data

Supplementary material related to this article can be found, in the online version, at doi:https://doi.org/10.1016/j.scienta.2020.109763.

References

Azeem, A., Wu, Y.Y., Xing, D.K., Javed, Q., Ullah, I., 2017. Photosynthetic response of two okra cultivars under salt stress and re-watering. J. Plant Interact. 12 (1), 67–77. https://doi.org/10.1080/17429145.2017.1279356.

Balsamo, R., Boak, M., Nagle, K., Peethambaran, B., Layton, B., 2015. Leaf biomechanical properties in *Arabidopsis thaliana* polysaccharide mutants affect drought survival. J. Biomech. 48 (15), 4124–4129. https://doi.org/10.1016/j.jbiomech.2015.10.016.

Bian, C.Y., Ma, C.J., Liu, X.H., Gao, C., Liu, Q.R., et al., 2016. Responses of winter wheat yield and water use efficiency to irrigation frequency and planting pattern. PLoS One 11 (5), e0154673. https://doi.org/10.1371/journal.pone.0154673.

Butscher, C., Huggenberger, P., 2009. Modeling the temporal variability of karst groundwater vulnerability, with implications for climate change. Environ. Sci. Technol. 43 (6), 1665–1669. https://doi.org/10.1021/es801613g.

Cruz, Y.C., Scarpa, A.L.M., Pereira, M.P., Castro, E.M., Pereira, F.J., 2019. Growth of *Typha domingensis* as related to leaf physiological and anatomical modifications under drought conditions. Acta Physiol. Plant. 41 (5), 1–9. https://doi.org/10.1007/s11738-019-2858-1.

Fernández, P.A., Roleda, M.Y., Hurd, C.L., 2015. Effects of ocean acidification on the photosynthetic performance, carbonic anhydrase activity and growth of the giant kelp *Macrocystis pyrifera*. Photosynth. Res. 124 (3), 293–304. https://doi.org/10.1007/s11120-015-0138-5.

Fila, G., Zeinalipour, N., Badeck, F.W., Delshad, M., Ghashghaie, J., 2019. Application of water-saving treatments reveals different adaptation strategies in three Iranian melon genotypes. Sci. Hortic. 256, 108518 https://doi.org/10.1016/j.scienta.2019.05.045.

Garcia-Navarro, J.C., Schulze, M., Friedrich, K.A., 2019. Measuring and modeling mass transport losses in proton exchange membrane water electrolyzers using electrochemical impedance spectroscopy. J. Power Sources 431, 189–204. https://doi.org/10.1016/j.jpowsour.2019.05.027.

Gaudin, R., Roux, S., Tisseyre, B., 2017. Linking the transpirable soil water content of a vineyard to predawn leaf water potential measurements. Agr. Water Manage. 182, 13–23. https://doi.org/10.1016/j.agwat.2016.12.006.

Guo, M., Pegoraro, A.F., Mao, A., Zhou, E.H., Arany, P.R., et al., 2017. Cell volume change through water efflux impacts cell stiffness and stem cell fate. P. Natl. Acad. Sci. U. S. A. 114 (41), E8618–E8627. https://doi.org/10.1073/pnas.1705179114.

He, C.Q., Tan, G.E., Liang, X., Du, W., Chen, Y.L., et al., 2010. Effect of Zn-tolerant bacterial strains on growth and Zn accumulation in *Orychophragmus violaceus*. Appl. Soil Ecol. 44, 1–5. https://doi.org/10.1016/j.apsoil.2009.07.003.

Javed, Q., Wu, Y.Y., Xing, D.K., Ullah, I., Azeem, A., et al., 2018. Salt-induced effects on growth and photosynthetic traits of *Orychophragmus violaceus* and its restoration through re-watering. Braz. J. Bot. 41 (1), 29–41. https://doi.org/10.1007/s40415-017-0432-x.

Jócsák, I., Végvári, G., Vozáry, E., 2019. Electrical impedance measurement on plants: a review with some insights to other fields. Theor. Exp. Plant Physiol. 31, 359–375. https://doi.org/10.1007/s40626-019-00152-y.

Kole, C., 2011. Wild Crop Relatives: Genomic and Breeding Resources-oilseeds. Springer, Berlin, Germany.

Li, D.S., Yao, J.Y., Liu, N., 2014. Review on physical information detection technology of plant leaves. J. China Univ. Metrol. 25 (3), 238–244. https://doi.org/10.3969/j.issn.1004—1540.2014.03.003 (in Chinese).

Lindén, H., Hagen, E., Łęski, S., Norheim, E.S., Pettersen, K.H., et al., 2016. LFPy: a tool for biophysical simulation of extracellular potentials generated by detailed model neurons. Front. Neuroinform. 7 (41), 1–15. https://doi.org/10.3389/fninf.2013.00041.

Luo, Y.Y., Zhao, X.Y., Qu, H., Zuo, X.A., Wang, S.K., et al., 2014. Photosynthetic performance and growth traits in *Pennisetum centrasiaticum* exposed to drought and rewatering under different soil nutrient regimes. Acta Physiol. Plant. 36 (2), 381–388. https://doi.org/10.1007/s11738-013-1419-2.

Rascio, A., Santis, G.D., Sorrentino, G., 2020. A low-cost method for phenotyping wilting and recovery of wheat leaves under heat stress using semi-automated image analysis. Plants 9 (6), 718. https://doi.org/10.3390/plants9060718.

Santesteban, L.G., Miranda, C., Marín, D., Sesma, B., Intrigliolo, D.S., et al., 2019. Discrimination ability of leaf and stem water potential at different times of the day through a meta-analysis in grapevine (*Vitis vinifera* L.). Agric. Water Manage 221, 202–210. https://doi.org/10.1016/j.agwat.2019.04.020.

Schönleber, M., Ivers-Tiffée, E., 2015. Approximability of impedance spectra by RC elements and implications for impedance analysis. Electrochem. Commun. 58, 15–19. https://doi.org/10.1016/j.elecom.2015.05.018.

Vaziriyeganeh, M., Lee, S.H., Zwiazek, J.J., 2018. Water transport properties of root cells contribute to salt tolerance in halophytic grasses *Poa juncifolia* and *Puccinellia nuttalliana*. Plant Sci. 276, 54–62. https://doi.org/10.1016/j.plantsci.2018.08.001.

Wang, R., Wu, Y.Y., Hang, H.T., Liu, Y., Xie, T.X., et al., 2014. *Orychophragmus violaceus*L., a marginal land-based plant for biodiesel feedstock: Heterogeneous catalysis, fuel properties, and potential. Energy Convers. Manage. 84, 497–502. https://doi.org/10.1016/j.enconman.2014.04.047.

Wilbur, K.M., Anderson, N.G., 1948. Electrometric and colorimetric determination of carbonic anhydrase. J. Biol. Chem. 176 (1), 147–154. http://www.jbc.org/content/176/1/147.

Wu, Y.Y., Xu, W.X., 2011. Effect of plant growth regulators on the growth of *Orychophragmus violaceus* plantlets in vitro. Planta Med. 77 (12), 1292–1293. https://doi.org/10.1055/s-0031-1282328.

Wu, Y.Y., Shi, Q.Q., Wang, K., Li, P.P., Xing, D.K., et al., 2011. An electrochemical approach coupled with Sb microelectrode to determine the activities of carbonic anhydrase in the plant leaves. In: Zeng, D. (Ed.), Future Intelligent Information

Systems, LNEE 86. Springer-Verlag, Berlin, Germany, pp. 87–94. https://doi.org/10.1007/978-3-642-19706-2_12.

Xing, D.K., Wu, Y.Y., 2012. Photosynthetic response of three climber plant species to osmotic stress induced by polyethylene glycol (PEG) 6000. Acta Physiol. Plant. 34 (2), 1659–1668. https://doi.org/10.1007/s11738-012-0961-7.

Xing, D.K., Wu, Y.Y., Fu, W.G., Li, Q.L., Hu, L.S., et al., 2016. Regulated deficit irrigation scheduling of *Orychophragmus violaceus* based on photosynthetic physiological response traits. T. ASABE 59 (6), 1853–1860. https://doi.org/10.13031/trans.59.11853.

Xing, D.K., Chen, X.L., Wu, Y.Y., Xu, X.J., Chen, Q., et al., 2019. Rapid prediction of the re-watering time point of *Orychophragmus violaceus* L. based on the online monitoring of electrophysiological indexes. Sci. Hortic. 256, 108642 https://doi.org/10.1016/j.scienta.2019.108642.

Zhang, C., Hicks, G.R., Raikhel, N.V., 2015a. Molecular composition of plant vacuoles: important but less understood regulations and roles of tonoplast lipids. Plants 4, 320–333. https://doi.org/10.3390/plants4020320.

Zhang, M., Wu, Y., Xing, D., Zhao, K., Yu, R., 2015b. Rapid measurement of drought resistance in plants based on electrophysiological properties. T. ASABE 58 (6), 1441–1446. https://doi.org/10.13031/trans.58.11022.